STRUCTURAL PROPERTIES OF GRAPHENE OXIDE COATINGS FROM DIFFERENT SHEETS SIZES

Nurul Huda Abu Bakar[1], Jamil Ismail[1], Kwok Feng Chong[1*]

[1]*Faculty of Industrial Sciences & Technology,*
Universiti Malaysia Pahang, Gambang, 26300, Kuantan, Malaysia

[*]Corresponding author: ckfeng@ump.edu.my

Abstract
The structural properties of different sizes of graphene oxide (GO) sheets were observed. It is worth to mention that smaller size GO sheets (ultrasonicated 10h) exhibits higher absorption intensity, and the absorption peak was shifted towards lower wavelength (~223 nm) due to the fragmentation of the GO sheets. It has caused an extension of a π-conjugated system, thereby enhance the absorption intensity and energy. After electrophoretic deposition (EPD), the coatings exhibit a reduction in the oxygen content with oxygen-related band (ORB) values of the larger GO sheets is higher than that of small size GO sheets. The surface morphology of both the coatings are homogenous and the layers adhered well to the underlying copper. However, larger GO sheets exhibit rougher and coarser morphology than that of small size GO sheets. It is reflected in the thickness measurement where the large size GO sheets exhibit thicker film (3.16 ± 0.01 μm) while small size GO sheets possess thinner film (1.95 ± 0.02 μm).

Keyword: Coating, Electrophoretic Deposition, Graphene oxide, Sheet size, Ultra-sonication

Introduction

There are increasing publications related to 2D carbon materials such as graphene. Graphene exists as a single atomic monolayer of graphite that possesses a unique combination of properties that are ideal for various application such as energy storage device (Zhang et al., 2013), anticorrosion coating (Cui et al., 2019; Kakaei, Esrafili, & Ehsani, 2019) as well as sensors (Pang et al., 2018). Due to its unique nature, graphene has extraordinary electrical properties such as high electron mobility (Böhm, 2014), excellent optical properties (Nair et al., 2008) and a remarkable mechanical property (Lee, Wei, Kysar, & Hone, 2008). Usually, a high-quality graphene was synthesized *via* 'bottom-up' approach, which is a chemical vapor deposition (CVD) method. The CVD involves the use of methane (CH_4) (Chen et al., 2011) or sodium ethoxide (C_2H_5ONa) (Raza et al., 2017) as a carbon precursor. The CVD graphene requires high temperature to enable decomposition of the hydrocarbon sources to produce thin, graphitic layers on the metal surfaces. The need for high temperature, pressure, and high vacuum environment limits the application of this method.

On the other hand, the electrophoretic deposition (EPD) method has more advantages as it can be executed at room temperature/environment, ambient pressure and low deposition temperature. It was reported that the optimum temperature for electrodeposition of graphene-based composite coating was determined as low as 45 °C (Jabbar et al., 2017). However, the disadvantage of applying EPD using pure graphene is they are insoluble in water and do not form a stable suspension. Therefore, the graphene derivative of graphene oxide (GO) is preferred because it has high dispersion ability which is attributed to its large number of oxygenated functional groups (epoxide, hydroxyl, carboxyl and carbonyl) (Dreyer, Park,

Bielawski, & Ruoff, 2010). The naturally negative charge of GO (from the oxygen functional groups at the edge and basal plane of the GO sheets) results in the formation of anodic EPD process.

Basically, a stable GO suspension is needed for a successful EPD process. Agglomeration and sedimentation of GO sheets in the suspension would produce uneven film, thereby deteriorating the film's performance. Hence, the ultra-sonication technique is widely used to disperse and exfoliate GO sheets into stable suspension. Also, the ultra-sonication parameters such as time and power play critical factors in determining the end size of the GO sheets. Previous study reported that longer ultra-sonication time promotes the breakage of GO sheets and accompanied by the reduction reaction, mainly by the elimination of carboxylic and carbonyl functional groups (Gonçalves et al., 2014). Another study showed that after 7h of sonication, the size of the GO sheets was reduced to ~100 nm as compared to 290 nm for 1h sonication (Bakar, Ali, Ismail, Algarni, & Chong, 2019).

Therefore, in this contribution, different size GO sheets by controlling the ultra-sonication time at 5 and 10 hours has been prepared. The GO dispersion was then electrophoretically deposited onto copper substrates to make EPD-GO coatings. The structural and morphological properties of the ultra-sonicated GO and the EPD-GO are evaluated.

Materials and Methods

Several flat copper substrates (purity 99.9 %) were purchased from Kimberly RD, Hong Kong. The substrates were cut into 10 mm × 100 mm × 400 mm and were cleaned with acetone in an ultrasonic bath. All the other chemicals used in this research were purchased from Sigma–Aldrich unless otherwise specified.

Preparation of Different Size GO Sheets

Prior to differentiate the GO sheets sizes, the GO precursor was synthesized *via* modified Hummers' method following previous report (Bakar et al., 2019). The as-synthesized GO was then dispersed in DI water to make up a concentration of 1.0 mg/mL. The GO dispersion was then divided into two different vials for 5h and 10h ultra-sonication using Bransonic CPX2800H (110 W, 40 kHz) to yield GO into different sheets sizes. They were termed as 5h-GO and 10h-GO throughout the discussion. Both were centrifuged at 6000 rpm before the EPD process in order to remove any un-exfoliated GO.

Electrophoretic Deposition (EPD)-GO

A two-electrode system was used for EPD with both anode and cathode were made of copper substrates. A potentiostat (PGSTAT101; Autolab by Metrohm) was used for the EPD process to supply +1.0V for 900 s until a uniform coating was obtained on the anode. The anodic EPD-GO samples were dried in an oven at 80 °C, overnight and labelled as 5h-GO/Cu and 10h-GO/Cu, respectively.

Characterizations

The optical properties of the ultrasonic-assisted GO dispersion were determined using UV-Visible spectrophotometer (THERMO SCIENTIFIC: Genesys 10S by Thermo Fisher). The functional groups of the EPD-GO coatings were determined by Fourier Transform Infrared Spectrometer (FTIR; Spectrum 100 by Perkin Elmer), in the range of 400 – 4000 cm^{-1}. The graphitic structure and crystallinity of the samples were investigated by Raman spectrometer (inVia Reflex by Renishaw) with 532 nm laser light source. The surface morphology was observed using field emission scanning electron microscope (FESEM) (JSM-7800 F by JEOL)

at 5.0 kV. Finally, the coating thickness was measured by a surface profiler (P-6 Stylus Profiler by KLA Tencor).

Results and Discussion

UV-Vis and absorption coefficient (α)

Figure 1 (a) shows the UV-Vis spectra of 5h-GO and 10h-GO dispersion. In **Figure 1(a)**, the 5h-GO spectrum displays a maximum absorption peak centered at 230 nm and a shoulder peak at about 302 nm attributed to $\pi \rightarrow \pi *$ and $n \rightarrow \pi *$ electronic transition of aromatic C=C and carbonyl C=O functional groups, respectively (Sahu et al., 2013). Interestingly, 10h-GO exhibits a higher absorption intensity and the absorption peak shifted towards a lower wavelength (~223 nm). It is suggested that prolonged ultra-sonication hour exfoliates and breaks the GO sheets into smaller sizes. The fragmentation causes an extension of a π-conjugated system, thereby enhance the absorption intensity and energy. Another possible outcome is breaking GO into smaller nanoparticles would involve the elimination of oxygen functional groups (COOH and C=O). Therefore, more hydrophobic materials are obtained due to the formation of -CH$_2$ bonds (Gonçalves et al., 2014). Overall, the GO dispersions were monitored closely during the sonication hours and it shows stable dispersions with no indication of coagulation even after keeping for several weeks (~32 weeks).

In the meantime, **Figure 1 (b)** shows the absorbance at 660 nm as a function of concentration for the 5h-GO and 10h-GO samples, respectively. The slopes of the lines indicated the absorption coefficients (α) and were estimated from the plots of absorbance, A *vs* concentrations, c according to Lambert-Beer law, $A = \alpha c l$ where l is constant liquid optical pathlength (Su, Lin, Chen, & Chen, 2014). The values were found to be 1.1034 and 1.3015 for 5h-GO and 10h-GO, respectively. A striking feature is that the absorption coefficient increases when the size of the GO sheets decreases. Apparently, the absorbance increases linearly with increasing concentration, indicating that the ultra-sonicated GO dispersion follows the Lambert-Beer law.
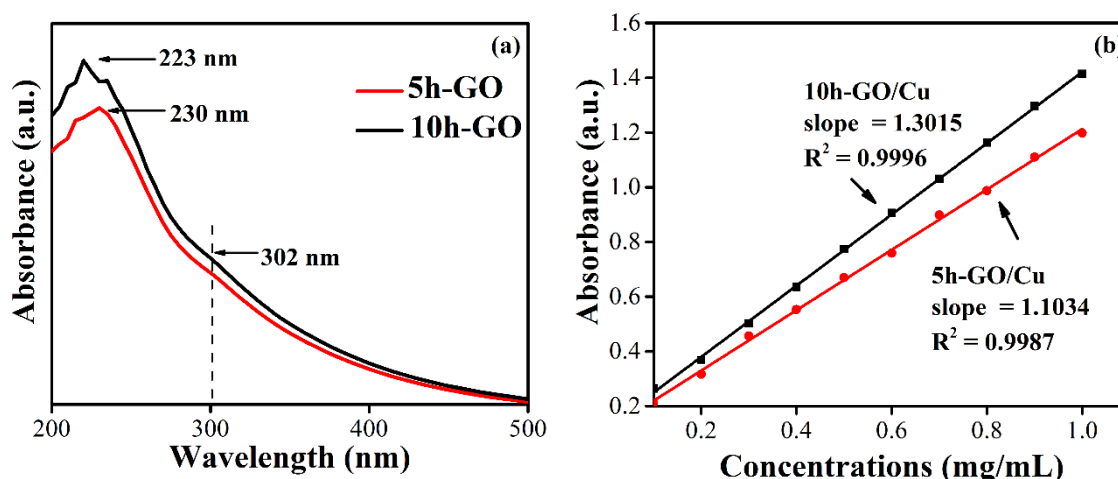
Figure 1 (a) UV-Vis spectra and **(b)** absorption coefficient (α) for 5h-GO and 10h-GO

Structural properties of EPD-GO

The 5h-GO and 10h-GO dispersion were electrophoretically deposited onto the copper surface. The deposits were characterized using FTIR spectroscopy in the range of 400 to 4000 cm^{-1}.

Figure 2 (a) shows the obtained spectra for 5h-GO/Cu and 10h-GO/Cu coatings. A broadband at 3434 cm^{-1} is attributed to stretching of the –OH functional groups on the GO surface. There is a significant reduction on the absorption of the –OH stretching vibrations for the 10h-GO/Cu sample.

Obviously, there is a disappearance of the characteristic band at ~1724 cm^{-1} suggesting the partial reduction of GO during EPD through oxidative decarboxylation process (An et al., 2010). Meanwhile, ~950 cm^{-1} band is epoxy mode while a broad area around 1200 cm^{-1} band is attributed to the C-O mode. For a better comparison, the oxygen-related band (ORB) was calculated for the 5h-GO/Cu and 10h-GO/Cu samples. The ORB was quantitatively determined by deconvoluted the bands into Gaussian peaks to obtain the peak areas. The aromatic C=C peak area was then substitute from the total area under the spectra and the ORB ratio was determined using Equation (1). The values were found to be 0.39 and 0.37, respectively. The findings indicate that the 10h-GO/Cu exhibits more oxygen reduction, thereby forming more hydrophobic surfaces.

$$\frac{A_{ORB}}{A_{total}} = \frac{A_{total} - A_{C=C}}{A_{total}} = ORB : total \qquad (1)$$

The Raman spectra measured at 532 nm for the coatings are presented in **Figure 2 (b)**. It is worth mentioning that the D and G bands do not shift as a function of the GO sheets size. The integrated area ratio of I_D/I_G was found to be 1.34 for 5h-GO/Cu and 1.37 for 10h-GO/Cu. The graphene crystallite size, L_a was also calculated from Equation (2) (Tuinstra & Koenig, 1970);

$$L_a = (2.4 \times 10^{-10}) \, \lambda_l^4 \, (I_D/I_G)^{-1} \qquad (2)$$

where L_a is the crystallite size and λ_l is the wavelength of the laser source (nm). The results show that graphene crystallite size for 5h-GO/Cu is 14.35 nm while the graphene crystallite size for 10h-GO/Cu is 14.03 nm. It is ascertained that the I_D/I_G ratio increases as the crystallite size decrease. Furthermore, the variation in intensity ratios of G and D band could be due to the change in the electronic conjugation state of GO. The result is consistent with the above mention findings where longer ultra-sonication hours promote the breakage of GO sheets into smaller sizes.

Surface morphology

Figure 3 (a) and **(b)** display the microscopic images of the EPD-GO coatings. The 5h-GO/Cu morphology is rougher and coarser as compared to that 10h-GO/Cu. It could be due to the larger GO sheets sizes and thicker GO layer. However, it can be observed that both coatings mimic the topology of the underlying copper substrates. It is attributed to the graphene's thinnest material characteristics and, therefore, it is almost entirely transparent (Raman & Tiwari, 2014). To add, the coatings are well-adhered to the copper surfaces as there were no delamination occurred. The thickness of the coatings was found to be 3.16 ± 0.01 µm for 5h-GO/Cu and 1.95 ± 0.02 µm for 10h-GO/Cu
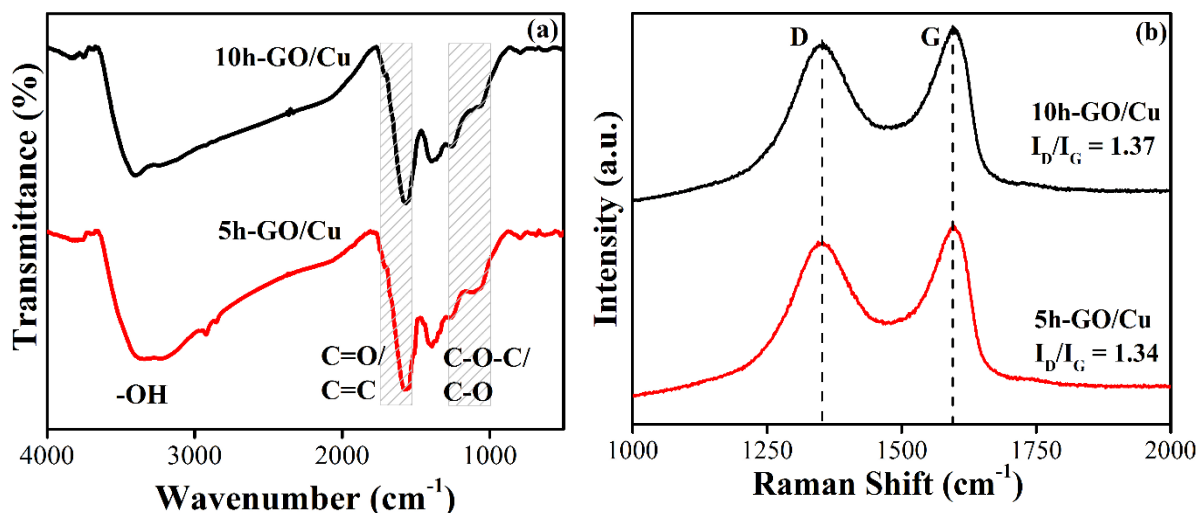
Figure 2 (a) FTIR spectra and **(b)** Raman measurement for 5h-GO/Cu and 10h-GO/Cu coatings
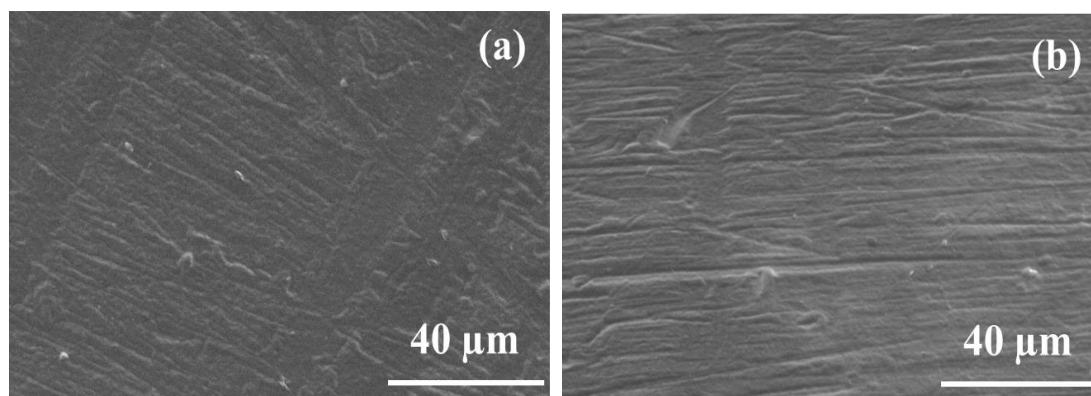
Figure 3 Comparison of surface morphologies for EPD-GO coatings **(a)** 5h-GO/Cu and **(b)** 10h-GO/Cu

Conclusion

Different GO sheets sizes have been successfully synthesized by simple ultra-sonication technique at 5h and 10h. The GO coatings from the small size GO sheets showed smooth and thinner coating as compared to the large size GO sheets with thickness measurement of 1.95 ± 0.02 µm. It is interesting to note that small size GO sheets experienced more oxygen reduction during EPD as calculated from ORB value. It could be suggested that more oxygen reduction causing the formation of graphene, thereby increase the hydrophobicity of the surfaces. In addition, it is expected that the GO coatings can be applied as corrosion-resistant material and provide better alternatives from conventional coatings. All the findings are summarized in **Table I** for better comparison.

Table 1 Summary of findings for different GO sheets sizes and the EPD-GO coatings

Samples	Absorption coefficient (α)	ORB	I_D/I_G	L_a (nm)
5h-GO/Cu	1.1034	0.39	1.34	14.35
10h-GO/Cu	1.3015	0.37	1.37	14.03

Acknowledgement

Conflict of interests

The authors declare no competing financial interest.

References

An, S. J., Zhu, Y., Lee, S. H., Stoller, M. D., Emilsson, T., Park, S., . . . Ruoff, R. S. (2010). Thin film fabrication and simultaneous anodic reduction of deposited graphene oxide platelets by electrophoretic deposition. *The Journal of Physical Chemistry Letters, 1*(8), 1259-1263.

Bakar, N. H. A., Ali, G. A., Ismail, J., Algarni, H., & Chong, K. F. (2019). Size-dependent corrosion behavior of graphene oxide coating. *Progress in Organic Coatings, 134*, 272-280.

Böhm, S. (2014). Graphene against corrosion. *Nature nanotechnology, 9*(10), 741.

Chen, S., Brown, L., Levendorf, M., Cai, W., Ju, S.-Y., Edgeworth, J., . . . Piner, R. D. (2011). Oxidation resistance of graphene-coated Cu and Cu/Ni alloy. *ACS nano, 5*(2), 1321-1327.

Cui, G., Bi, Z., Zhang, R., Liu, J., Yu, X., & Li, Z. (2019). A comprehensive review on graphene-based anti-corrosive coatings. *Chemical Engineering Journal*.

Dreyer, D. R., Park, S., Bielawski, C. W., & Ruoff, R. S. (2010). The chemistry of graphene oxide. *Chemical Society Reviews, 39*(1), 228-240.

Gonçalves, G., Vila, M., Bdikin, I., De Andrés, A., Emami, N., Ferreira, R. A., . . . Marques, P. A. (2014). Breakdown into nanoscale of graphene oxide: confined hot spot atomic reduction and fragmentation. *Scientific reports, 4*, 6735.

Jabbar, A., Yasin, G., Khan, W. Q., Anwar, M. Y., Korai, R. M., Nizam, M. N., & Muhyodin, G. (2017). Electrochemical deposition of nickel graphene composite coatings: effect of deposition temperature on its surface morphology and corrosion resistance. *RSC Advances, 7*(49), 31100-31109.

Kakaei, K., Esrafili, M. D., & Ehsani, A. (2019). Graphene and Anticorrosive Properties *Interface Science and Technology, 27*, 303-337

Lee, C., Wei, X., Kysar, J. W., & Hone, J. (2008). Measurement of the elastic properties and intrinsic strength of monolayer graphene. *science, 321*(5887), 385-388.

Nair, R. R., Blake, P., Grigorenko, A. N., Novoselov, K. S., Booth, T. J., Stauber, T., . . . Geim, A. K. (2008). Fine structure constant defines visual transparency of graphene. *science, 320*(5881), 1308-1308.

Pang, Y., Jian, J., Tu, T., Yang, Z., Ling, J., Li, Y., . . . Yang, Y. (2018). Wearable humidity sensor based on porous graphene network for respiration monitoring. *Biosensors and Bioelectronics, 116*, 123-129.

Raman, R. S., & Tiwari, A. (2014). Graphene: The thinnest known coating for corrosion protection. *Jom, 66*(4), 637-642.

Raza, M. A., Ali, A., Ghauri, F. A., Aslam, A., Yaqoob, K., Wasay, A., & Raffi, M. (2017). Electrochemical behavior of graphene coatings deposited on copper metal by electrophoretic deposition and chemical vapor deposition. *Surface and Coatings Technology, 332*, 112-119.

Sahu, S. C., Samantara, A. K., Seth, M., Parwaiz, S., Singh, B. P., Rath, P. C., & Jena, B. K. (2013). A facile electrochemical approach for development of highly corrosion protective coatings using graphene nanosheets. *Electrochemistry Communications, 32*, 22-26.

Su, R., Lin, S. F., Chen, D. Q., & Chen, G. H. (2014). Study on the absorption coefficient of reduced graphene oxide dispersion. *The Journal of Physical Chemistry C, 118*(23), 12520-12525.

Tuinstra, F., & Koenig, J. L. (1970). Raman spectrum of graphite. *The Journal of Chemical Physics, 53*(3), 1126-1130.

Zhang, F., Zhang, T., Yang, X., Zhang, L., Leng, K., Huang, Y., & Chen, Y. (2013). A high-performance supercapacitor-battery hybrid energy storage device based on graphene-enhanced electrode materials with ultrahigh energy density. *Energy & Environmental Science, 6*(5), 1623-1632.